

JAAS

Accepted Manuscript

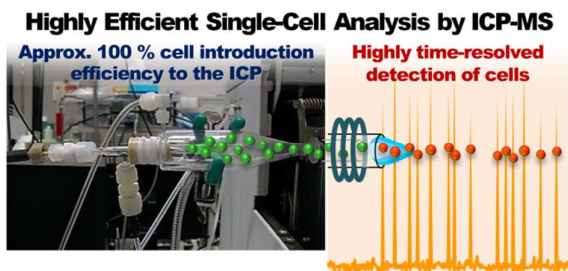


This is an *Accepted Manuscript*, which has been through the Royal Society of Chemistry peer review process and has been accepted for publication.

Accepted Manuscripts are published online shortly after acceptance, before technical editing, formatting and proof reading. Using this free service, authors can make their results available to the community, in citable form, before we publish the edited article. We will replace this *Accepted Manuscript* with the edited and formatted *Advance Article* as soon as it is available.

You can find more information about *Accepted Manuscripts* in the [Information for Authors](#).

Please note that technical editing may introduce minor changes to the text and/or graphics, which may alter content. The journal's standard [Terms & Conditions](#) and the [Ethical guidelines](#) still apply. In no event shall the Royal Society of Chemistry be held responsible for any errors or omissions in this *Accepted Manuscript* or any consequences arising from the use of any information it contains.



Highly efficient single-cell elemental analysis of microbial cells was achieved using a developed inductively-coupled plasma mass spectrometry (ICP-MS) system with approximately 100 % cell introduction efficiency and high time resolution.

Highly efficient single-cell analysis of microbial cells by time-resolved inductively-coupled plasma mass spectrometry

Cite this: DOI: 10.1039/x0xx00000x

Received 00th January 2012,
Accepted 00th January 2012

DOI: 10.1039/x0xx00000x

www.rsc.org/

Shin-ichi Miyashita,^{*a} Alexander S. Groombridge,^b Shin-ichiro Fujii,^a Ayumi Minoda,^c Akiko Takatsu,^a Akiharu Hioki,^a Koichi Chiba^a and Kazumi Inagaki^a

To realise highly efficient single-cell analysis of microbial cells by time-resolved inductively-coupled plasma mass spectrometry (ICP-MS), we developed the modified high efficiency cell introduction system (HECIS), consisting of a large-bore high performance concentric nebulizer (LB-HPCN) with a centre capillary tube of 150 μm inner diameter and a custom-made small-volume (15 cm^3) on-axis spray chamber that uses a sheath gas flow near the chamber exit to suppress cell deposition. We also assembled an external ion pulse counting unit to directly read the ion pulse current from the electron multiplier of the ICP-MS via a function generator with no dead time, in order to obtain data with sufficiently high time resolution (*i.e.*, 0.05 ms–1 ms). As compared to a conventional ICP-MS working at its minimum integration time (10 ms), this assembly led to more than *ca.* 13-fold higher signal-to-background ratios for ^{31}P , and made higher throughput of cells to the plasma more feasible. By using the modified HECIS and the external ion pulse counting unit for determination of the cell introduction efficiencies of different-sized unicellular microbes, including yeast (*Saccharomyces cerevisiae*), cyanobacterium (*Synechocystis* sp. PCC 6803), red algae (*Cyanidioschyzon merolae* 10D and *Galdieria sulphuraria*), and green alga (*Chlamydomonas reinhardtii* CC-125), it was revealed that their cell introduction efficiencies ranged from 86 % (for *C. reinhardtii* CC-125 with a mean cell diameter of 6.4 μm) to *ca.* 100 % (for other microbes with mean cell diameters of 2.0 μm –3.0 μm), implying that by use of the ICP-MS system, the cell introduction efficiencies are able to reach approximately 100 % and tend to decrease with increasing cell sizes (at least more than 3.1 μm in mean diameter). A wide range of biologically important elements, such as C, Mg, Al, P, S, K, Ca, Cr, Mn, Fe, and Zn, were tested for reasonable detection using the ICP-MS system. Results likely corresponding to separate cell events were obtained for some elements present in each microbe.

Introduction

White biotechnology is the application of biotechnology for industrial purposes, including manufacturing, alternative energy to replace fossil fuels, and biomaterials. It includes the utilization of cells or components of cells such as enzymes to clean up polluted environments and generate industrially useful products. For example, a unicellular green microalga *Euglena* can clean polluted water by taking up various contaminants from the water and digesting them in their bodies.¹ *Euglena* can also synthesize oil inside its body that can be used as a biofuel.^{1,2} In such cell processes, many elements are likely to play important roles as catalysts for various enzymes. Elemental composition and respective distribution in a single cell can serve as indicators for cell health and growth states. These parameters critically impact the efficiency of cells in a

biotechnological process because each cell contributes to product yield and dead, inactive or weakly active cells will limit this productivity. Thus, single-cell elemental analysis needs to be involved in the evaluation and control of such cell processes.

In recent years, single-cell elemental analysis using inductively-coupled plasma (ICP) spectrometers, such as ICP optical emission spectrometry (ICP-OES) and ICP mass spectrometry (ICP-MS), has gained substantial interest in the biochemical and metallomics fields.^{3–8} When cells are directly introduced into the plasma, ion plumes of the cells are generated after their vaporization. If one cell is introduced over the duration of the ion plume generation (0.2 ms–0.4 ms, dependent on plasma gas flow)^{6,9} and the integration time per data point is shorter than the duration of the ion plume generation, the ion plumes corresponding to individual cells

(*i.e.* single-cell events in the plasma) can be detected as current spike signals above the background signal in the detector without overlap. The major challenging issue in the single-cell analyses using commercial ICP spectrometers described so far are the use of grossly inefficient sample introduction systems via liquid and suspension nebulization, typically <1 % as previously noted,^{5,8} and the limit on achievable time resolution due to instrument operating software, typically 1 ms–10 ms.⁹

Previously, we have developed a high efficiency cell introduction system (HECIS),¹⁰ consisting of the high performance concentric nebulizer (HPCN)^{11–14} with a centre capillary tube of 110 μm inner diameter and a custom-made small-volume (*i.e.* lower dead volume) on-axis spray chamber (15 cm^3) that used a sheath gas flow near the chamber exit for suppression of cell deposition; it was successfully used in elemental analysis of individual yeast cells (*Saccharomyces cerevisiae*) by time-resolved ICP-MS.¹⁰ A reproducible cell introduction efficiency of 75.0 ± 4.7 % was achieved, mostly due to the high proportion of small droplets (less than 10 μm in diameter) generated by the nebulizer, which leads to a lower background noise level.

However, the cell introduction efficiency was not close to 100 %, likely due to loss of cells during introduction into the ICP. Moreover, the cell throughput was limited to *ca.* 13 cells per second to statistically prevent overlap of separate cell events in the resultant time-resolved spectra; this is a result of the limiting time resolution of the instrument used being 10 ms, longer than the duration of the ion plume. At this integration time, the maximum signal-to-background (S/B) ratio obtainable was not high enough, potentially missing the current spikes corresponding to some of the cells, thus giving erroneous measurements of the cell introduction efficiency. In addition, cell introduction efficiencies of other types of unicellular microbes different in diameter from yeast (*ca.* 4 μm) have not been tested thus far. The cell introduction efficiencies of larger-sized microbial cells are expected to decrease due to increased deposition in the sample introduction system, it would be necessary to make improvements to the HECIS to account for this.

In this study, we realised highly efficient single-cell analysis of microbial cells of different sizes by time-resolved ICP-MS through the following approaches. Firstly, for reducing the loss of cells to walls inside the spray chamber, and to accept a wider range of different-sized cells (from 2.0 μm to 6.4 μm in mean diameter), the HPCN used in the HECIS was altered to have a large-bore central capillary (LB-HPCN) and a small-volume (15 cm^3) on-axis spray chamber with a longer total length and shorter inner tube length, still utilizing a sheath gas flow. Next, for obtaining data with higher time resolution (*i.e.*, 0.05 ms–1 ms), an external ion pulse counting unit was assembled for direct reading of the ion pulse current from the electron multiplier of the ICP-MS.

Experimental

Sample introduction apparatus

Sample introduction was carried out using the HECIS¹⁰ after its modification to allow for different-sized cells, as described hereinbelow. A schematic diagram of the modified HECIS is shown in Fig. 1. It was composed of the LB-HPCN having a triple tube concentric structure with a centre capillary tube of 150 μm inner diameter (the original being 110 μm inner diameter) and the newly-designed small-volume (15 cm^3) on-axis spray chamber with longer total length of 11.1 cm and shorter inner tube length of 3.2 cm, utilizing a sheath gas flow in an area seemingly critical for cell deposition. The chamber used was selected based on performance comparison results with the original one (10.7 cm total chamber length and 4.0 cm inner tube length) (Fig. S1), because of the higher S/B ratios of ²⁵Mg, ³¹P, ⁵⁵Mn, and ⁶⁶Zn (exceptionally slightly lower those of ³⁴S and ³⁹K) obtained in the time-resolved mass spectra, which would have resulted from: (1) the background signals were decreased because droplets containing a single cell could fly for a longer distance inside the chamber to more vaporize (*i.e.* the solvent of the droplets being more evaporated) and/or (2) the possible breaking of cells of varying degrees by collisions with walls inside the chamber could be prevented due to the longer distance. The latter (2) could contribute to the former (1) because decrease of background signals likely corresponds to equal or lower breaking of the cells into the chamber.

The pump used for sample introduction into the ICP-MS was a double plunger type high pressure pump (LC10-AD; Shimadzu, Japan). The cell suspension was introduced via an inert 6-port PEEK flow injector (V200; Flom Co. Ltd., Japan) equipped with a 30- μL sample loop. All sample tubing used was made from PTFE (0.33 mm inner diameter) to prevent cell adsorption to tubing walls as much as possible. Similar to our previous study,¹⁰ a dilute sodium chloride (NaCl) solution was added to the cell suspension immediately before analysis, and also to the cell flowing liquid to reduce cell adsorption, allowing consecutive measurements without fear of significant contamination from previous measurements.

ICP-MS instrumentation

All measurements were carried out with a quadrupole mass analyser Agilent 7500a ICP-MS (Agilent Technologies, CA, USA). The minimum integration time setting on the software was 10 ms. At this integration time, each cell event was detected at one data point, and the probability of two cell events being detected at one data point at 10 $\mu\text{L min}^{-1}$ flow rate (*i.e.* two cells overlapping during the integration time) was 1.8 %.¹⁰ The ICP-MS was externally equipped with an ion pulse counting unit (C8855-01; Hamamatsu Photonics K.K., Japan) for directly reading the ion pulse current from the electron multiplier of the ICP-MS via a function generator (HP 8112A; Hewlett-Packard Co., CA, USA) without the intrinsic dead time of the detector system, enabling measurement of a single data point at the shorter integration time of 0.05 ms or 0.1 ms and detection of each cell event with multiple data points.

Typical operating conditions are given in Table 1. The scanning mode was set to peak hopping with no repeats. Since the actual measurement time was determined by the sample

software attached to the ion pulse counting unit, the measurement time of the ICP-MS was set to the maximum value of 1000 s just for convenience. The ICP-MS was tuned daily using a cell flowing liquid prepared from caesium (Cs) standard solution ($0.3 \mu\text{g L}^{-1}$ in 0.1 % w/v NaCl), for maximum sensitivity at m/z of 133.

The number of ions in the plume, sampled by the sampler cone and then admitted into the MS, likely depends on the initial position of the cell when it first enters the ICP and the opening of the sampler cone. Since the radial position of the plume in the central channel of the ICP is random, ICP torch with smaller injector tube diameter of 1.5 mm (previously 2.5-mm tube used¹⁰) was employed for reducing the ICP-MS spike intensity variance. This was inspired by Ho *et al.*⁸ who performed single-cell analysis of *Chlorella vulgaris* cells and single-particle analysis of gold nano-particles using an ICP torch with an injector tube diameter of 2.5 mm and observed the broadening of the ICP-MS spike intensity distribution, probably related to uncertainty in the portion of the ion plume sampled.

Reagents and materials

Water used throughout was prepared by a Milli-Q water purification system ($18 \text{ M}\Omega \text{ cm}^{-1}$ resistivity; Nihon Millipore Kogyo K.K., Japan). NaCl stock solution (5 % w/v, total 100 mL) was prepared from NaCl solid (Suprapur® grade; Merck, Darmstadt, Germany) with water. The cell flowing liquid (containing Cs) used for tuning the ICP-MS was made from a 1000 mg L^{-1} single-element standard solution (Kanto Chemical Industries Ltd., Japan).

Polypropylene single-use Eppendorf micropipette tips used were thoroughly cleaned by immersion in 3 mol L^{-1} HNO_3 (electronic grade, Kanto Chemical) for a week, followed by rinsing with water five times and drying in a clean desiccator. 15 mL and 50 mL polypropylene centrifuge tubes (IWAKI) used for preparing cell suspensions were purchased from Asahi Glass Co. Ltd., Japan.

Cell culture

The following wild-type strains of unicellular microbes were used as model organisms: yeast (*S. cerevisiae*), cyanobacterium (*Synechocystis* sp. PCC 6803), red algae (*Cyanidioschyzon merolae* 10D and *Galdieria sulphuraria*), and green alga (*Chlamydomonas reinhardtii* CC-125). All microbes except for yeast were cultured in 50 mL of culture media in three glass vessels, under the previously-described conditions with a continuous light exposure of $70 \mu\text{E m}^{-2} \text{ s}^{-1}$ in the laboratory environment. *Synechocystis* sp. PCC 6803 was grown to mid-log phase in BG-11 medium with 1 % CO_2 bubbling at $30 \text{ }^\circ\text{C}$.¹⁵ *C. merolae* 10D was grown to mid-log phase in Allen's medium with air-bubbling at $42 \text{ }^\circ\text{C}$.¹⁶ *G. sulphuraria* was grown to late-log phase in modified $2\times$ Allen's medium with 5 % CO_2 bubbling at $42 \text{ }^\circ\text{C}$.¹⁶ *C. reinhardtii* CC-125 was grown to late-log phase in TAP medium at $30 \text{ }^\circ\text{C}$.¹⁷

Cell suspension

The cell suspension (50 mL) was collected from one glass vessel of each microbe into a 50 mL centrifuge tube, and the cells were harvested by centrifugation at 2380 g for 8 min at ambient temperature and rinsed with 10 mL of water three times. The cells in each tube were suspended in 10 mL of 0.1 % (w/v) NaCl and diluted with the same salt solution to make its cell number density approximately 800 cells per $10 \mu\text{L}$ ($8.0 \times 10^4 \text{ cells mL}^{-1}$) to give a total volume of 10 mL for immediate use, and then the accurate cell number density was determined by at least three repeated cell counts with a haemocytometer.

An aliquot (10 mL) of yeast cell suspension including 800 cells per $10 \mu\text{L}$ was prepared daily from commercial bakery yeast, containing only the dried cells of *S. cerevisiae* (Shirakami Kodama Dry Yeast; Sala Akita Shirakami Corp., Japan), as similarly in our previous study.¹⁰ The concentration of NaCl was adjusted to 0.1 % (w/v) at last.

The cell suspension prepared was not only subjected to cell size distribution analysis by laser diffraction, but also directly introduced into the plasma of the ICP-MS as an aerosol through the modified HECIS for time-resolved ICP-MS measurement. Since 0.1 % (w/v) NaCl solution is not isotonic, and is in fact quite hypotonic, the time the cells were left suspended in NaCl solution was kept to a minimum (<30 min) to prevent significant transport of ions across the cell membranes. Even so, the NaCl solution may have depressed cell concentrations of biologically relevant metals. The cell suspension prepared was agitated before each measurement.

Cell counting

The cell suspension prepared was appropriately diluted with 0.1 % (w/v) NaCl in a 15 mL centrifuge tube and then subjected to cell counting using single-use haemocytometers (DHC-N01 C-Chip; Digital Bio Inc., Seoul, South Korea) under an optical microscope (IX70-S1F; Olympus Corporation, Japan) at 400-fold magnification. The error in the cell counts was then calculated by relative standard deviation (RSD), on average being around 5 % for the same suspension with three repeats.

Cell size distribution

The cell size distribution of each microbe was recorded using a laser diffraction system (Aerotrac LDSA-SPR, model 7340; Nikkiso Co., Japan), with the suspension contained in a quartz cell on a magnetic stirrer. The laser focus distance was 100 mm, and the measurement range of cell diameter was from 0.5 μm to 355 μm . Data on the distribution for each suspension was the average of five tests with ten repeats each, recorded as volume percentage assuming spherical cells. *C. merolae* 10D cells are not completely spherical; therefore, inaccuracies may be present in their measurements.

Fig. 2 shows the typical size distribution of the microbial cells in the prepared cell suspension. The mean cell diameters are: 2.0 μm for *Synechocystis* sp. PCC 6803, 2.4 μm for *C. merolae* 10D, 2.4 μm –3.1 μm (median, 2.8 μm) for yeast (*S. cerevisiae*), 3.0 μm for *G. sulphuraria*, and 6.4 μm for *C. reinhardtii* CC-125. The mean diameters of *Synechocystis* sp. PCC 6803 and yeast cells reflect their typical cell diameters of

1 about 2 μm ¹⁸ and 3 μm (for a small cell),¹⁹ respectively. The
2 size distribution of *C. reinhardtii* CC-125 cells had a broad
3 range from 2.0 μm to 26.3 μm , which can cover the reported
4 mean cell diameter, for example, varying from 4.5 μm –5 μm ²⁰
5 to 8.5 μm –9.1 μm .²¹ The larger diameters of more than
6 approximately 9 μm might correspond to cell clusters in the
7 suspension (Fig. S2); they are dissipated into single cells
8 contained within separate droplets upon nebulization due to the
9 high gas flow acting upon the liquid stream. Therefore, they are
10 likely not present in the time-resolved mass spectrum.

11 Cell introduction efficiency

12 Cell introduction efficiency was calculated by comparing the
13 number of spikes (spike frequency) for ³¹P in a 60 s
14 measurement at 10 $\mu\text{L min}^{-1}$ (*i.e.*, 10 μL), with the number of
15 cells (cell frequency) per 10 μL (counted with a
16 haemocytometer) of the prepared cell suspension.

17 Results and discussion

18 Improvement of the S/B ratio and the cell throughput into the 19 plasma

20 For improving the S/B ratios of cell events and the cell
21 throughput into the plasma in single-cell analysis by time-
22 resolved ICP-MS, we assembled an external ion pulse counting
23 unit for direct reading of the ion pulse current from the electron
24 multiplier of the ICP-MS. As a result, we obtained sufficiently
25 high time resolution (*i.e.*, 0.05 ms–0.1 ms to measure a single
26 data point). As a cell event in the plasma lasts *ca.* 0.2 ms–0.4
27 ms,^{6,9} the obtained time resolution is enough to realise high-
28 throughput single-cell analysis. In addition, when compared to
29 a conventional ICP-MS working at its minimum integration
30 time (10 ms), it led to more than *ca.* 13-fold higher S/B ratios
31 for ³¹P due to the reduced background noise, and made a higher
32 cell throughput more feasible, as mentioned below in detail.

33 The S/B ratio can be improved by having a shorter
34 integration time per data point (*i.e.* higher time resolution) than
35 the duration of ion plume generation.⁹ When the integration
36 time is much longer than the duration of ion plume generation,
37 spike signals in response to cell events become low due to
38 averaging with the background signals in the integration.
39 Meanwhile, when the integration time is shorter than the
40 duration of ion plume generation, these losses can be
41 minimized. As can be seen in Fig. 3, by shortening the
42 integration time of our ICP-MS system to 0.1 ms, the S/B ratios
43 in the measurement of ³¹P in microbial cells were considerably
44 improved by 12.9- (*C. reinhardtii* CC-125) to 22.2-fold
45 (*Synechocystis* sp. PCC 6803) compared to those obtained at an
46 integration time of 10 ms. This improvement enabled us to
47 clearly distinguish spikes corresponding to separate cell events
48 from background spikes, and thereby reduce possible counting
49 loss of the cell peaks in the calculation of cell introduction
50 efficiency. The interrelationship between integration times
51 (0.05 ms–10 ms), number of data points per spike, probability
52 of two cells overlapping with each other, and S/B ratio for ³¹P

on each integration time is summarized in Fig. 4, taking *C.*
merolae 10D as an example.

Cell throughput can be increased by increasing the time
resolution, but the maximum cell throughput is limited by the
duration of ion plume generation (*ca.* 0.2 ms–0.4 ms^{6,9}). Olesik
et al. calculated the probabilities of detecting signals from one
particle or more than one within an integration time per data
point, when the duration is *ca.* 0.4 ms.⁹ They indicate that the
probability of detecting signals from more than one particle can
be reduced by increasing the time resolution, but the number of
particles entering the plasma must be limited to keep the
probability of the signals overlapping with each other
acceptably low. In a conventional ICP-MS system (without the
external ion pulse counting unit) working at its minimum
integration time (10 ms), the cell throughput was limited to *ca.*
13 cells per second without overlapping of cell events,¹⁰ but
now in the developed system, it could be further increased
probably up to its theoretical limitation of *ca.* 500 cells–1000
cells per second,^{9,22} thereby contributing to acquisition of more
reliable data on the cells. In fact, the cell throughput was
experimentally confirmed to achieve 274 cells per second when
ca. 16500 yeast cells per 10 μL were introduced into ICP-MS at
a flow rate of 10 $\mu\text{L min}^{-1}$. In this connection, the linear
relationship found between the spike frequency for ³¹P and cell
number density in the cell suspensions (*ca.* 200 cells–16500
cells per 10 μL) is shown in Fig. S3. The number of spikes per
10 μL in the mass spectrum for increasing the number of cells
per 10 μL gave a linear trend with an R^2 value of 0.9989. These
results indicate that high cell throughput can be achieved
without overlapping of cell events.

Cell introduction efficiency

For improving the cell introduction efficiency into the plasma
in single-cell analysis by time-resolved ICP-MS, we refined the
HECIS to have the LB-HPCN and a 15 cm³ on-axis spray
chamber with longer total length and shorter inner tube length
utilizing a sheath gas flow. The modified HECIS accepted a
wide range of different-sized cells (from 2.0 μm to 6.4 μm in
mean diameter) and enabled us to achieve cell introduction
efficiencies of 103.2 \pm 1.9 % (*Synechocystis* sp. PCC 6803),
107.9 \pm 1.2 % (*C. merolae* 10D), 100.9 \pm 6.9 % (*S. cerevisiae*),
108.2 \pm 2.0 % (*G. sulphuraria*), and 85.6 \pm 9.2 % (*C.*
reinhardtii CC-125) when monitoring the ³¹P⁺ ion. This
improvement is due to reduction in the loss of cells during
introduction into the ICP. We previously reported that a
reproducible cell introduction efficiency of yeast cells (*S.*
cerevisiae) was 75.0 \pm 4.7 % when monitoring the ³¹P⁺ ion.¹⁰
Compared to not only the previous study but also other
studies^{22,23} reporting cell introduction efficiencies of <30 %, the
efficiencies of more than 86 % achieved in this study are
significantly high.

As mentioned above, we obtained the cell introduction
efficiencies of 86 %–108 % for several microbes with mean
cell diameters of 2.0 μm –6.4 μm . However, it must be noted
here that the probability of cell organelle measurement has not
been excluded. In the case of yeast, for example, the ICP-MS

spike intensities for P in single cells were around 1000 counts when measured at the minimum integration time of 0.05 ms. If the cells were partially broken up during the process of nebulization or by collisions with walls inside the spray chamber, and single organelles released from the broken cells had more than one-fourth of the total P in single cells, spikes from the single organelles (corresponding to intensities of >250 counts) might have been counted as those from single cells, which could possibly lead to overestimation of the cell introduction efficiency. Another point to note is that the cell introduction efficiencies decreased with increasing cell sizes; that is, the efficiency only for *C. reinhardtii* CC-125 with a mean cell diameter of 6.4 μm was 86 % while those for other microbes with mean cell diameters of 2.0 μm –3.0 μm were ca. 100%. Possible reasons for this are (1) that some of the larger-sized cells were more continually lost to the walls inside the spray chamber, (2) that much less ionization of the larger-sized cells took place inside the plasma, and (3) that two cell events overlapped with each other during the integration time. In fact, the chamber showed visible deposits of cells at the coned section of the chamber near the exit after frequent use for three weeks, despite the use of a flow of sheath gas along the walls of the coned section in order to minimize this deposition effect. These potential problems need to be faced through effective countermeasures and will be addressed more thoroughly in the future.

Cell measurement efficiency

Cell measurement efficiency can be guided by multiplying “cell introduction efficiency into the plasma” (*i.e.* cell introduction percentage) by “cell throughput into the plasma” (*i.e.* number of cells introduced per second). If the probability of two cells overlapping with each other during the same integration time is ignorable, the cell throughput can be also defined as “cell transmission efficiency to the detector”. To realise highly efficient single-cell analysis, sufficiently-high cell measurement efficiency is required.

Cell introduction systems of ICP spectrometers can be classified into two groups: nebulizing systems^{5–8,10,23} such as that applied in this study, and droplet dispensing systems^{19,24–26} (*i.e.* an ink-jet printing system). Regarding droplet dispensing systems, the cell introduction efficiency can theoretically be 100 %, but the cell throughput is normally low due to avoiding agglomeration of cells in single droplets and generating stable droplets at a relatively low frequency (below 200 Hz in triple pulse mode²⁴), resulting in low cell measurement efficiency. In addition, S/B ratios of cell events are decreased by large background signals due to large-sized droplets (minimum ca. 20 μm in diameter). Recently, Shigeta *et al.*¹⁹ applied a micro-droplet dispensing unit tandem with a desolvation system to introduce selenized yeast cells into the plasma. Uniformly-sized droplets of 23 μm in diameter were successfully dispensed with the rate of 50 Hz, and the cell introduction efficiency of 100 % was achieved. However, it was noted that the number density of cells in a suspended solution was diluted to 1 cell or 5 cells per 100 droplets to avoid agglomeration of cells in single droplets;

therefore, the cell throughput calculated was only 0.5 cell or 2.5 cells per second, respectively. In this study, we used our original nebulizing system and then obtained the cell introduction efficiency of at most ca. 100 % for different-sized cells (from 2.0 μm to 3.0 μm in mean diameter) and the relatively higher cell throughput (theoretically ca. 500 cells–1000 cells per second and experimentally at least 274 cells per second confirmed in this time), resulting in extremely high cell measurement efficiency.

Elemental analysis of single cells by time-resolved ICP-MS

By time-resolved ICP-MS using the modified HECIS, spike signals corresponding to microbial cell events were successfully detected for P (Fig. 5) and some other elements on introduction of the cell suspension. The $^{31}\text{P}^+$ ions gave the largest spike frequency, and their spike signals were mostly separated from background signals in the time-resolved mass spectrum, and so the current work using ICP-MS was based around it.

As a result of comparing the distributions of the spike intensities in the ICP-MS spectrum of ^{31}P and the cell volume within each microbe examined, the trend of the distribution of the background-corrected spike intensities was relatively similar to that of the microbial cell volume distribution calculated from the diameter measured by the laser diffraction system (Fig. 6). These results imply that spike intensity for the elements in single cells strongly correlates with the volume of the cells, as P is mainly present as a structural component of the nucleic acids such as RNA and DNA, and then in the phospholipids of cell membranes and the polyphosphate esters such as ADP and ATP.

The RSDs of the average spike intensities of ^{31}P , along with other representative elements, corresponding to the maximum frequency are summarized in Table 2, taking *Synechocystis* sp. PCC 6803, *C. merolae* 10D, and *C. reinhardtii* CC-125 as examples. The RSDs of the triplicate measurements ranged from 8 % to 21 % for P (2 %–23 % for Mg, 6 %–21 % for S, and 5 %–14 % for Mn) due to variability in the cell size, showing good reproducibility. These results indicate that highly-sensitive elemental analysis of single cells was achieved.

A wide range of biologically important elements were tested for reasonable detection using the developed ICP-MS system. Results likely corresponding to separate cell events were obtained for six elements (^{25}Mg , ^{27}Al , ^{31}P , ^{34}S , ^{39}K , and ^{55}Mn) in *Synechocystis* sp. PCC 6803, six elements (^{13}C , ^{25}Mg , ^{31}P , ^{34}S , ^{55}Mn , and ^{64}Zn) in yeast (*S. cerevisiae*), eight elements (^{13}C , ^{25}Mg , ^{31}P , ^{34}S , ^{39}K , ^{55}Mn , and ^{66}Zn) in *C. merolae* 10D, seven elements (^{13}C , ^{25}Mg , ^{31}P , ^{44}Ca , ^{52}Cr , ^{54}Fe , and ^{55}Mn) in *G. sulphuraria*, and seven elements (^{13}C , ^{25}Mg , ^{27}Al , ^{31}P , ^{34}S , ^{55}Mn , and ^{66}Zn) in *C. reinhardtii* CC-125. Example mass spectra for the elements in *C. merolae* 10D are shown in Fig. 7. However, the desired results were not obtained for ^{13}C and ^{66}Zn in *Synechocystis* sp. PCC 6803, ^{27}Al in yeast and *C. merolae* 10D, ^{39}K and ^{63}Cu in *G. sulphuraria*, and ^{39}K in *C. reinhardtii* CC-125 because of their low contents in the cells, or the effects of high background signals.

Conclusions

We developed the modified HECIS and assembled an external ion pulse counting unit to directly read the ion pulse current from the electron multiplier of the ICP-MS. Consequently, we successfully obtained a very short integration time of 0.05 ms–0.1 ms. As compared to a conventional ICP-MS system working at its minimum integration time (10 ms), it lead to more than *ca.* 13-fold higher S/B ratios for ^{31}P and, and made higher throughput of cells to the plasma more feasible. By using the developed ICP-MS system for determination of the cell introduction efficiencies of different-sized unicellular microbes in single-cell analysis, it was revealed that their cell introduction efficiencies ranged from 86 % (for *C. reinhardtii* CC-125 with a mean cell diameter of 6.4 μm) to *ca.* 100 % (for other microbes with mean cell diameters of 2.0 μm –3.0 μm), implying that by use of this system, the cell introduction efficiencies are able to reach approximately 100 %, and tend to decrease with increasing cell sizes (at least more than 3.1 μm in mean diameter). A wide range of biologically important elements were tested for reasonable detection using the developed ICP-MS system and, consequently, results likely corresponding to separate cell events were obtained for some elements present in each microbe.

In future work, we will focus on single-cell elemental analysis of (1) individual organelles isolated from cultured microbial or plant cells in order to obtain information about the localization of elements in cells and (2) more larger-sized cells (like *Euglena gracilis* Z with a mean cell diameter of 17.7 μm) as compared to those handled in this study. Indeed, we have already attempted single-cell analysis of *Euglena* cells, but washing and handling of the cells were quite difficult because they are fragile (mostly due to absence of cell wall) and thus presumably unable to survive the processes of centrifugation and nebulization. Single-cell analysis of such large-sized and/or fragile cells is still challenging to be implemented.

Acknowledgements

The authors express sincere gratitude to S.T. Japan, Inc. and Mr Masaaki Abe for supporting the present research. This work was partly supported by Grant-in-Aid for Scientific Research (C) (No. 24550112) from the Japan Society for the Promotion of Science.

Notes and references

^a National Metrology Institute of Japan (NMIJ), National Institute of Advanced Industrial Science and Technology (AIST), 1-1-1 Umezono, Tsukuba, Ibaraki 305-8563, Japan. Fax: +81 29 861 6889; Tel: +81 29 861 6889; E-mail: shinichi-miyashita@aist.go.jp

^b Nano Doctoral Training Centre, The Cavendish Laboratory, The University of Cambridge, CB3 0HE, England.

^c Faculty of Life and Environmental Sciences, University of Tsukuba, 1-1-1 Tennodai, Tsukuba, Japan.

† Electronic Supplementary Information (ESI) available: Figure S1. See DOI: 10.1039/b000000x/

- 1 T. V. Ramachandra, M. D. Madhaba, S. Shilpia and N. V. Joshi, *Renew. Sust. Energ. Rev.*, 2013, **21**, 767.
- 2 S. Tucci, R. Vacula, J. Krajcovic, P. Proksch and W. Martin, *J. Eukaryot. Microbiol.*, 2010, **57**, 63.
- 3 H. Haraguchi, *J. Anal. At. Spectrom.*, 2004, **19**, 5.
- 4 Y. Lin, R. Trouillon, G. Safina and A. G. Ewing, *Anal. Chem.*, 2011, **83**, 4369.
- 5 T. Nomizu, S. Kaneco, T. Tanaka, D. Ito, H. Kawaguchi and B. T. Vallee, *Anal. Chem.*, 1994, **66**, 3000.
- 6 S. D. Tanner, D. R. Bandura, O. Ornatsky, V. I. Baranov, M. Nitz and M. A. Winnik, *Pure Appl. Chem.*, 2008, **80**, 2627.
- 7 F. Li, D. W. Armstrong and R. S. Houk, *Anal. Chem.*, 2005, **77**, 1407.
- 8 K. S. Ho and W. T. Chan, *J. Anal. At. Spectrom.*, 2010, **25**, 1114.
- 9 J. W. Olesick and P. J. Gray, *J. Anal. At. Spectrom.*, 2012, **27**, 1143.
- 10 A. S. Groombridge, S. Miyashita, S. Fujii, K. Nagasawa, T. Okahashi, M. Ohata, T. Umemura, A. Takatsu, K. Inagaki and K. Chiba, *Anal. Sci.*, 2013, **29**, 597.
- 11 K. Inagaki, S. Fujii, A. Takatsu and K. Chiba, *J. Anal. At. Spectrom.*, 2011, **26**, 623.
- 12 Y. Takasaki, K. Inagaki, A. Sabarudin, S. Fujii, D. Iwahata, A. Takatsu, K. Chiba and T. Umemura, *Talanta*, 2011, **87**, 24.
- 13 S. Fujii, K. Inagaki, A. Takatsu, T. Yarita and K. Chiba, *J. Chromatogr. A*, 2009, **1216**, 7488.
- 14 A. S. Groombridge, K. Inagaki, S. Fujii, K. Nagasawa, T. Okahashi, A. Takatsu and K. Chiba, *J. Anal. At. Spectrom.*, 2012, **27**, 1787.
- 15 Y. Shimura, Y. Shiraiwa and I. Suzuki, *Plant Cell Physiol.*, 2012, **53**, 1255.
- 16 A. Minoda, R. Sakagami, F. Yagisawa, K. Tsuneyoshi and K. Tanaka, *Plant Cell Physiol.*, 2004, **45**, 667.
- 17 S. Miyashita, S. Fujiwara, M. Tsuzuki and T. Kaise, *Biosci. Biotechnol. Biochem.*, 2011, **75**, 522.
- 18 M. Aoki, M. Tsuzuki and N. Sato, *BMC Res. Notes*, 2012, **5**, 98.
- 19 K. Shigeta, G. Koellensperger, E. Rampler, H. Traub, L. Rottmann, U. Panne, A. Okino and N. Jakubowski, *J. Anal. At. Spectrom.*, 2013, **28**, 637.
- 20 H. Morlon, C. Fortin, C. Adam and J. Garnier-Laplace, *Environ. Toxicol. Chem.*, 2006, **25**, 1408.
- 21 J. Kropat, A. Hong-Hermesdorf, D. Casero, P. Ent, M. Castruita, M. Pellegrini, S. S. Merchant and D. Malasarn, *Plant J.*, 2011, **66**, 770.
- 22 S. C. Bendall, G. P. Nolan, M. Roederer and P. K. Chattopadhyay, *Trends Immunol.*, 2012, **33**, 323.
- 23 D. R. Bandura, V. I. Baranov, O. I. Ornatsky, A. Antonov, R. Kinach, X. Lou, S. Pavlov, S. Vorobiev, J. E. Dick and S. D. Tanner, *Anal. Chem.*, 2009, **81**, 6813.
- 24 K. Shigeta, H. Traub, U. Panne, A. Okino, L. Rottmann and N. Jakubowski, *J. Anal. At. Spectrom.*, 2013, **28**, 646.
- 25 S. Gschwind, L. Flamigni, J. Koch, O. Borovinskaya, S. Groh, K. Niemax and D. Gunther, *J. Anal. At. Spectrom.*, 2011, **26**, 1166.
- 26 B. Franze, I. Strengge and C. Engelhard, *J. Anal. At. Spectrom.*, 2012, **27**, 1074.

Table 1 Typical operating conditions of (a) ICP-MS externally equipped with (b) an ion pulse counting unit

Parameter	Setting
(a) ICP-MS	
Plasma conditions	
Rf power	1.6 kW
Plasma gas flow rate	15 L min ⁻¹
Auxiliary gas flow rate	0.9 L min ⁻¹
Nebulizer gas flow rate	1.03 L min ⁻¹
Spray chamber sheath gas flow rate	0.25 L min ⁻¹
Sampling depth	7.0 mm
Data acquisition	
Scanning mode	Peak hopping
Data points per peak	1
Integration time	10 s
Measurement time	1000 s
(b) Ion pulse counting unit	
Gate time (synonymous with integration time)	0.05 ms, 0.1 ms, 1 ms, or 10 ms
Measurement points	100000
Measurement time	5 s (for gate time of 0.05 ms) 10 s (for gate time of 0.1 ms) 30 s–60 s (for gate times of 1 ms and 10 ms)

Table 2 Typical RSDs (%) of the average spike intensities of the representative elements (^{25}Mg , ^{31}P , ^{34}S , and ^{55}Mn) corresponding to the maximum frequency in the triplicate time-resolved ICP-MS measurements of microbial cells with 0.1 ms integration time, taking *Synechocystis* sp. PCC 6803, *C. merolae* 10D, and *C. reinhardtii* CC-125 as examples

Element	<i>Synechocystis</i> sp. PCC 6803	<i>C. merolae</i> 10D	<i>C. reinhardtii</i> CC-125
^{25}Mg	1.7 %	4.5 %	23.0 %
^{31}P	7.6 %	9.5 %	21.0 %
^{34}S	20.7 %	13.2 %	5.9 %
^{55}Mn	6.7 %	14.2 %	5.4 %

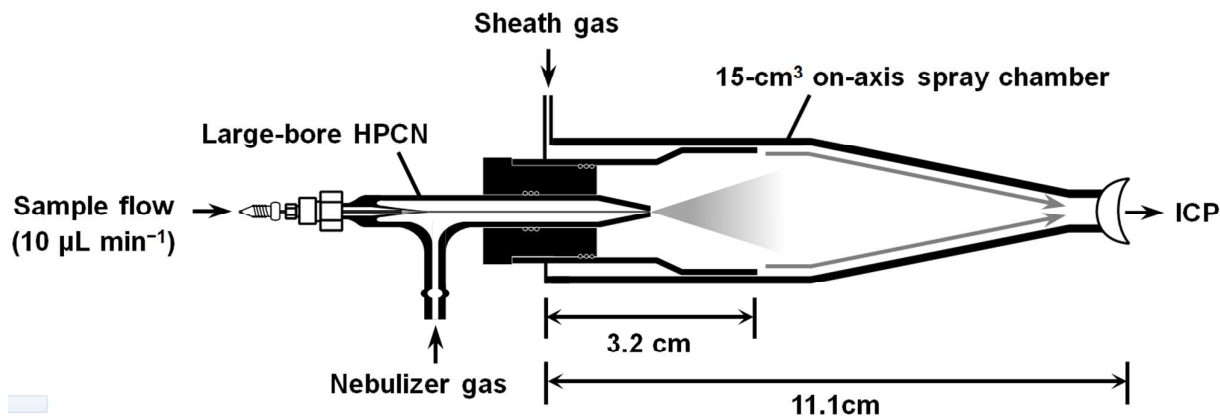


Fig. 1 A schematic diagram of the modified HECIS, consisting of the large-bore HPCN with an internal capillary of 150 µm inner diameter and a 15-cm³ on-axis spray chamber with total length of 11.1 cm and inner tube length of 3.2 cm utilizing a sheath gas flow.

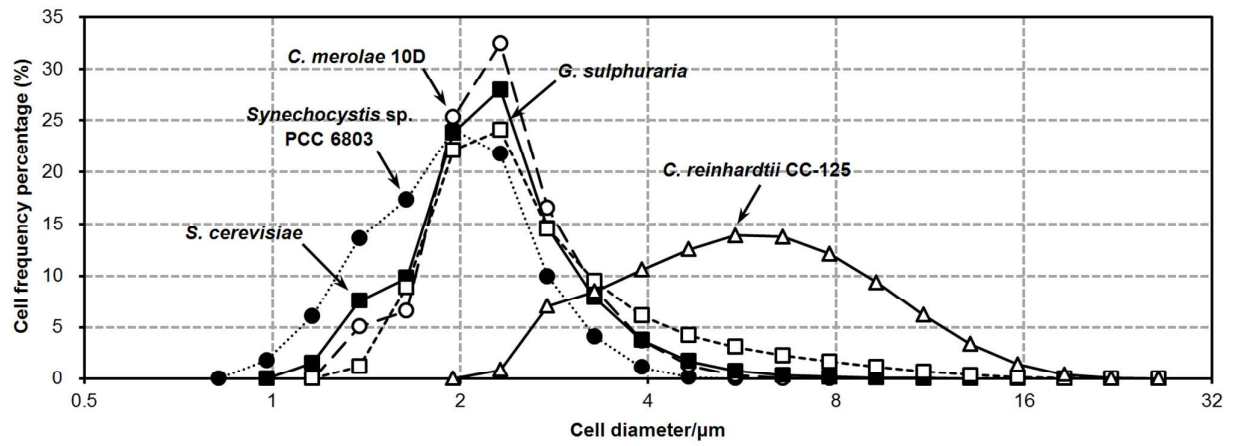


Fig. 2 Cell size distributions of microbial cells by frequency percentage.

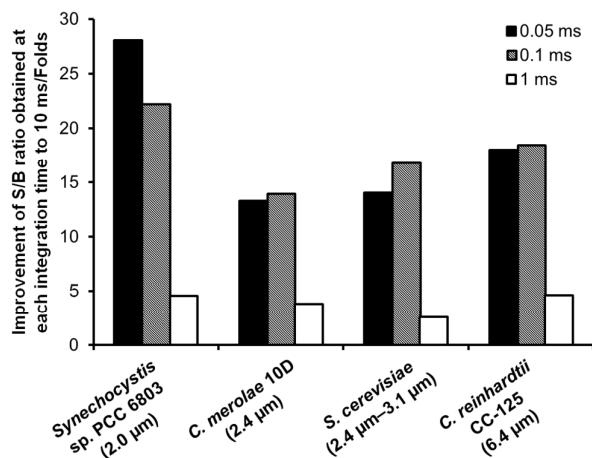


Fig. 3 Improvement of the typical S/B ratios for ^{31}P in the time-resolved ICP-MS measurements of *Synechocystis* sp. PCC 6803 (mean cell diameter, 2.0 μm), *C. merolae* 10D (2.4 μm), *S. cerevisiae* (2.4 μm –3.1 μm), and *C. reinhardtii* CC-125 cells (6.4 μm) by shortening the integration time of our ICP-MS system from 10 ms to 1 ms or 0.1 ms.

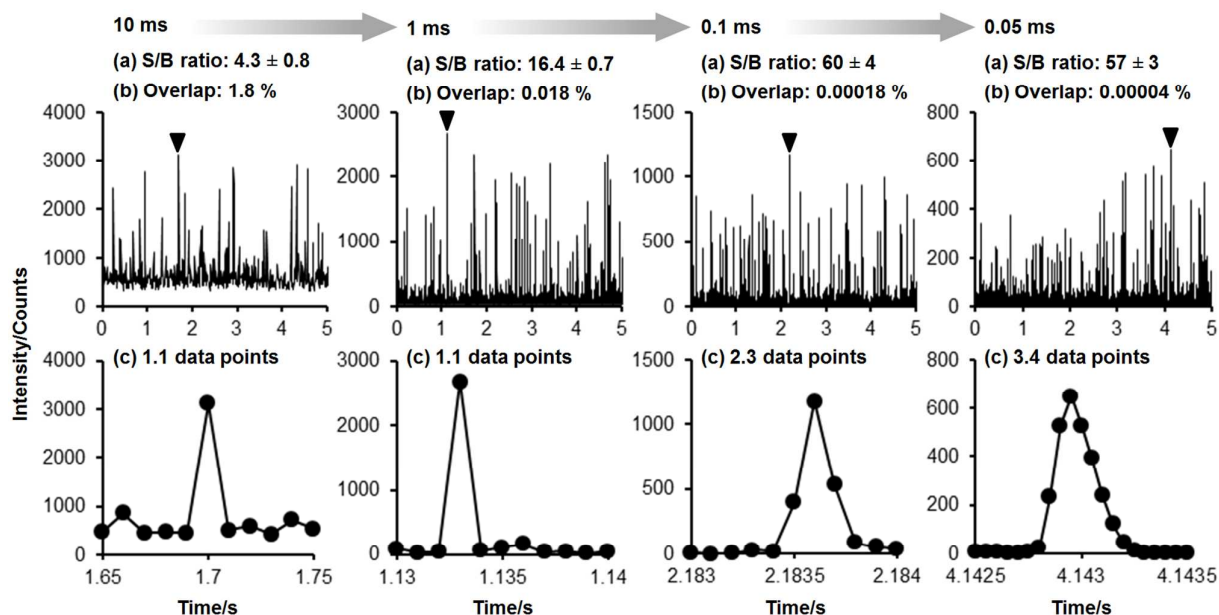


Fig. 4 Interrelationship between integration times ranging from 0.05 ms to 10 ms, (a) S/B ratio for ^{31}P (mean \pm SD of triplicate measurements) on each integration time, (b) probability of two cells overlapping each other (*ca.* 800 cells per 10 μL being introduced into the plasma at a flow rate of 10 $\mu\text{L min}^{-1}$, therefore 0.13 cells per integration time being introduced), and (c) average number of data points per spike counted using three sets of 5 s measurement data, taking *C. merolae* 10D as an example. Each upper graph represents the time-resolved mass spectrum ($^{31}\text{P}^+$) of microbial cell dispersed solution measured by ICP-MS, and each lower graph displays the enlarged figure from the black arrow-marked peak in the corresponding upper graph.

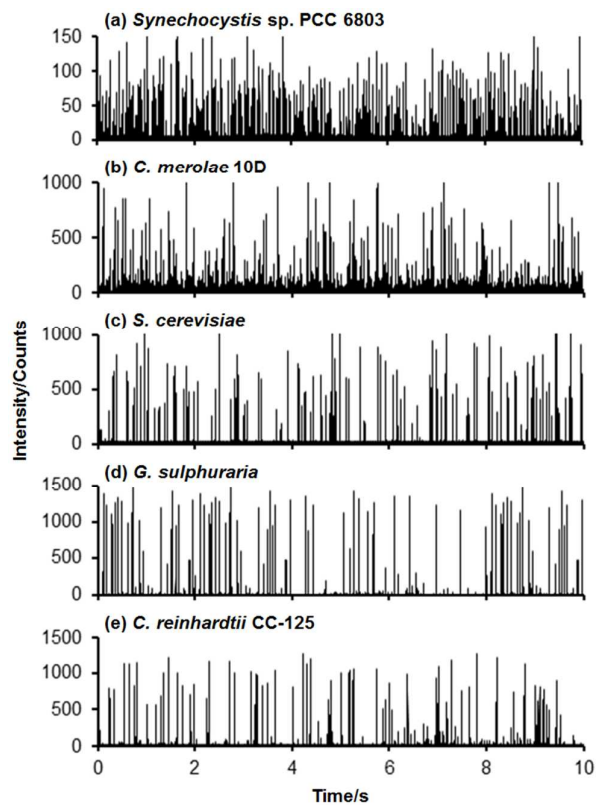


Fig. 5 Time-resolved mass spectra ($^{31}\text{P}^+$) of microbial cell dispersed solution measured by ICP-MS (integration time: 0.1 ms). (a) *Synechocystis* sp. PCC 6803; (b) *C. merolae* 10D; (c) *S. cerevisiae*; (d) *G. sulphuraria*, (e) *C. reinhardtii* CC-125.

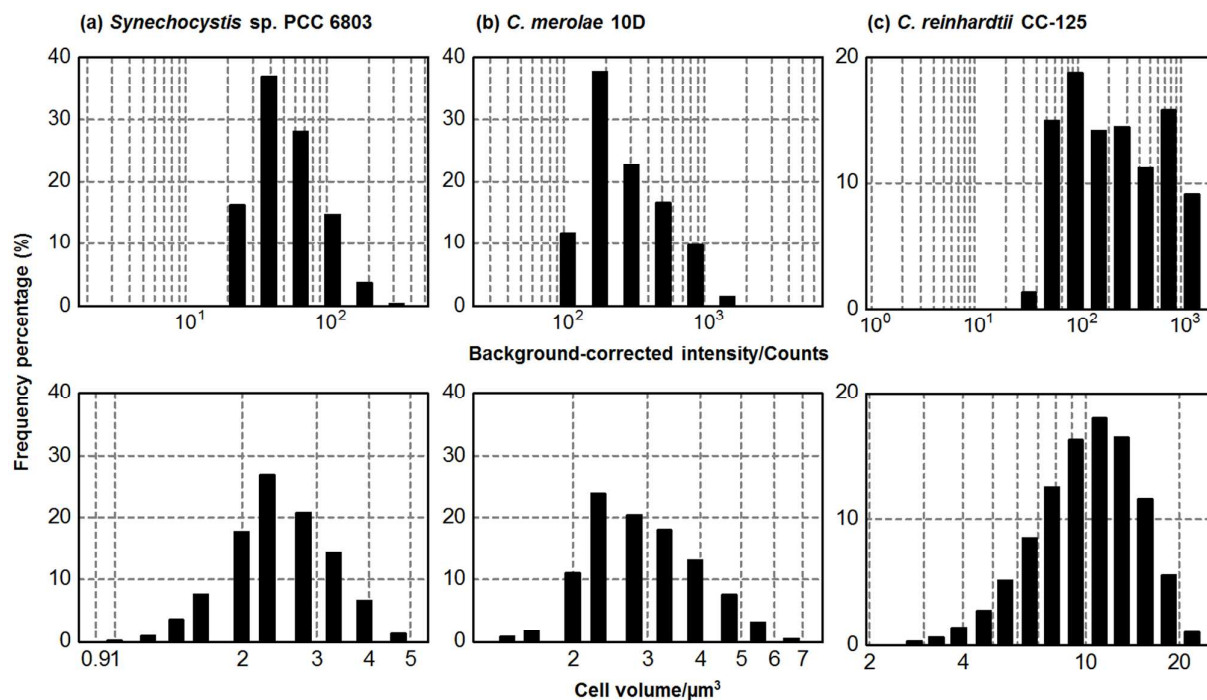


Fig. 6 Frequency distributions of the background-corrected spike intensities in the ICP-MS spectrum of $^{31}\text{P}^+$ obtained with 0.1 ms integration time (each upper graph) and the microbial cell volumes calculated from the diameter measured by the laser diffraction system (each lower graph). (a) *Synechocystis* sp. PCC 6803; (b) *C. merolae* 10D; (c) *C. reinhardtii* CC-125.

 1
2
3
4
5
6
7
8
9
10
11
12
13
14
15
16
17
18
19
20
21
22
23
24
25
26
27
28
29
30
31
32
33
34
35
36
37
38
39
40
41
42
43
44
45
46
47
48
49
50
51
52
53
54
55
56
57
58
59
60

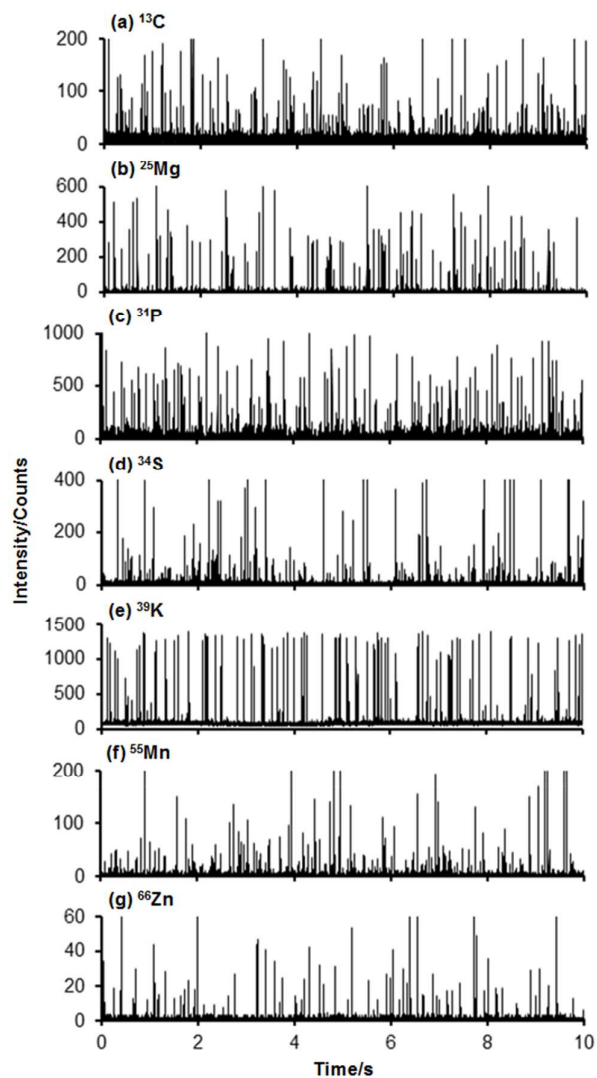


Fig. 7 Time-resolved mass spectra of *C. merolae* 10D cell dispersed solution measured by ICP-MS (integration time: 0.1 ms). (a) ^{13}C ; (b) ^{25}Mg ; (c) ^{31}P ; (d) ^{34}S ; (e) ^{39}K ; (f) ^{55}Mn ; (g) ^{66}Zn .